Placental homing peptide guides HIF1α-silenced exosomes conjugates for targeted enhancement of invasion of trophoblast cells

FANGRONG CHEN, HUI CEN, DONGRUI MAO and RONG FENG

Department of Obstetrics, Hainan General Hospital (Hainan Affiliated Hospital of Hainan Medical University), Haikou, Hainan 570311, P.R. China

Received March 9, 2023; Accepted April 21, 2023

DOI: 10.3892/mmr.2023.13022

Abstract. There is a current lack of availability of therapeutics to treat Preeclampsia (PE), primarily due to the risk of harm to the fetus. Hypoxia-inducible factor-1α (HIF1α) is highly expressed in trophoblast cells and suppresses their invasive ability. Extensive studies have confirmed the positive effects of mesenchymal stem cell (MSC)-derived exosomes on PE. The aim of the present study was to develop a method for targeted delivery of HIF1α-silenced exosomes to the placenta. HIF1α was overexpressed in JEG-3 cells. Then, the glucose uptake, lactate production, proliferation and invasion of HIF1α-elevated JEG-3 cells were detected. Exosomal membrane protein lysosome-associated membrane glycoprotein 2b and placental homing peptide CCGKRK gene sequence amplified by PCR were conjugated using short hairpin RNA-HIF1α (sh-HIF1α) sequence (exo-pep-sh-HIF1α), which were then transfected into MSCs cultured *in vitro*. Exosomes were isolated from the supernatant of the aforementioned MSCs and identified by determining the size and exosomal markers. Finally, the invasion ability of MSCs-derived exosomes treated JEG-3 cells were detected using Transwell assays. HIF1α was demonstrated to remarkably promote the uptake of glucose and the production of lactate in JEG-3 cells. In addition, high levels of HIF1α facilitated the proliferation of JEG-3 cells, while suppressing their invasion ability. Bone marrow derived MSCs were cultured *in vitro* and exosomes were successfully isolated from these cells. Exo-pep-sh-HIF1α significantly reduced placental HIF1α expression, and induced significant enhancement of placental invasion. Overall, placental homing peptide-guided HIF1α-silenced exosomes effectively facilitated the invasion of placental trophoblasts, which could be used for the targeted delivery of payloads to the placenta and serve as a novel placenta-specific therapeutic approach.

Correspondence to: Professor Hui Cen, Department of Obstetrics, Hainan General Hospital (Hainan Affiliated Hospital of Hainan Medical University), 19 Xiuhua Road, Haikou, Hainan 570311, P.R. China
E-mail: ch13976918410@126.com

Key words: preeclampsia, exosomes, placental homing peptide, hypoxia-inducible factor-1α, invasion

Introduction

Preeclampsia (PE) is a significant pregnancy-related disorder affecting 3 to 5% of pregnant women globally, marked by hypertension and proteinuria, appearing after 20 weeks of gestation (1). PE has been the third leading cause of maternal and neonatal morbidity and mortality with >60,000 mortalities in pregnant women with PE annually across the world (2,3). Currently, there are still no effective therapies for PE beyond delivery of the placenta (4,5). Despite ongoing research, the etiology of PE is not fully understood. However, studies have linked inappropriate remodeling of spiral arteries, immune dysregulation, inadequate trophoblastic invasion and endothelial damage to this condition (3,6,7).

MSCs display a capacity of potential self-renewal, broad differentiation potential, low immunogenicity and readily accessible properties, which offer MSCs advantages over other cell-based therapies (8,9). Moreover, factors secreted by MSCs have been correlated with angiogenesis and trophoblast formation, and can maintain successful pregnancy (10-12). However, the molecular mechanisms are still unclear. MSCs perform their therapeutic roles through paracrine mechanism. Exosomes are small extracellular vesicles that range from 30-100 nm in size and contain various biomolecules including nucleic acids, lipids, proteins, mRNA, miRNA and other non-coding RNAs (13). Exosomes derived from MSCs (MSC-Ex) can alleviate liver fibrosis, acute and chronic kidney injury, myocardial ischemia/reperfusion damage and acute tubular injury (14-16).

Exosomes have gained a lot of attention as a potential method for delivering therapeutics due to their non-immunogenicity and non-toxicity (17). Exosomes can be genetically engineered or their surface chemically modified to specifically target cells or tissues, allowing them to accumulate in tumor tissues (18). This enables more precise and targeted delivery of therapeutics. The tumor-targeting capability of exosomes was conferred by linking lysosome-associated membrane glycoprotein 2b (LAMP-2B), a well-characterized exosomal membrane protein (19), to internalizing arginine-glycine-aspartic acid

(CRGDKGPDC), which is widely recognized as an efficient cell membrane penetration peptide targeting αvβ3 integrins and neuropilin-1 (NRP-1) receptors (20). The CCG ligand (CCGKRK) has also shown selectivity towards placental tissue in mice (21). To the best of our knowledge, there is currently no study that has attempted to conjugate CCGKRK to LAMP-2B in order to enable exosomes target the placenta.

It is hypothesized that uteroplacental ischemia/hypoxia caused by impaired trophoblast invasion and uterine spiral arteriole remodeling is one of the leading causes of PE (6). During the first trimester of pregnancy, trophoblast cells are known to proliferate and survive in a hypoxic environment, which is beneficial for mural trophectoderm proliferation and spiral artery remodeling (22). Thus, during the initial phase of embryonic development, hypoxia-inducible factor-1α (HIF1α), an important transcription factor in placental development, is highly expressed in in trophoblast subpopulations. However, sustained hypoxia or HIF1α expression after 9 weeks of gestation will lead trophoblast cells to fail to differentiate from a proliferative to an invasive phenotype, shallow invasion of the trophoblasts and insufficient myometrial spiral artery transformation, which is strongly associated with early-onset PE (23,24). Therefore, HIF1α deletion might facilitate trophoblast invasion.

The present research is dedicated to exploring whether short hairpin RNA (shRNA)-HIF1α (sh-HIF1α) carried by MSC-Ex can effectively enhance the invasion ability of placental cells by conjugating sh-HIF1α-CCGKRK to LAMP-2B, thus providing a potential new therapeutic option for the prevention or treatment of PE (25). MSCs exosomes were used as a cell-based carrier for sh-HIF1α in the present study.

Materials and methods

JEG-3 cells culture. JEG-3 cells (ATCC; cat. no. HTB-36) were cultured in DMEM (cat. no. 10313039) adding 10% FBS (cat. no. 16140071) as well as 1% penicillin/streptomycin (cat. no. 15140122) (Gibco; Thermo Fisher Scientific, Inc.) under atmospheric oxygen tension (~21%) and 5% CO_2 at 37˚C.

Vector construction and lentiviral infection. HIF1α-overexpressing lentivirus (GV492-HIF1α) was constructed based on human HIF1α sequences from the Ensembl database (www.ensembl.org, Ensembl gene: ENSG00000100644) and synthesized by Shanghai GeneChem Co., Ltd. A 3rd generation system was used to package the lentivirus. The vectors (100 nM) and packaging plasmids (vector:packaging vector:envelope ratio, 10:3:1) were co-transfected into $1x10^6$ 293T cells (The Cell Bank of Type Culture Collection of The Chinese Academy of Sciences) using Lipofectamine® 2000 (Invitrogen; Thermo Fisher Scientific, Inc.) at 37˚C for 8 h. The lentivirus-HIF1α and negative control lentivirus (empty vector) were collected and filtered through a 0.45 μM filter 3 days after transfection. JEG-3 cells were then seeded in six-well plates at a density of $1x10^5$ cells/well and cultured at 37˚C in 5% CO_2. The JEG-3 cells were transduced with lentiviral vectors at a multiplicity of infection (MOI) of 10 at 37˚C for 8 h, followed by replacement with fresh medium. JEG-3 cells were grown for 48 h and subsequently treated with puromycin (1 μg/ml) for 48 h to select stably transduced cells and 0.5 μg/ml puromycin was used for maintenance. Subsequently, transduction efficiency was determined using immunofluorescence microscopy, and the expression of HIF1α was detected using quantitative PCR and western blotting.

Reverse transcription-quantitative PCR (RT-qPCR). RNA-iSo PluS (cat. no. 9109; Takara Bio, Inc.) was used to isolate total RNA from JEG-3 cells and MSC-Ex. cDNA was produced by cDNA Synthesis SuperMix (cat. no. 11119ES60; Shanghai Yeasen Biotechnology Co., Ltd.). The reverse transcription procedure was as follows: 25˚C for 5 min; 42˚C for 30 min; and 85˚C for 5 min. The cDNA was subjected to qPCR using SYBR Green qPCR Mix (cat. no. HY-K0501A; MedChemExpress) using the ABI 7500 Real-Time PCR system (Thermo Fisher Scientific, Inc.). The following ingredients were used to a total of 20 μl: cDNA (1 μl), SYBR Premix ex Taq (2X; 10 μl), reverse primer (10 μM; 0.4 μl), forward primer (10 μM; 0.4 μl) and double-distilled water (to 20 μl). Amplifications were performed following the procedure of a two-step method (95˚C for 30 sec; 1 cycle at 95˚C for 10 sec followed by 95˚C for 10 sec; 60˚C for 30 sec and 40 cycles; and melting curve stage). Relative HIF1α expression was normalized to GAPDH mRNA level and calculated via the $2^{-\Delta\Delta Cq}$ method (26). The sequences of primers used were as follows: GAPDH forward 5'-GGGAGCCAAAAGGGTCAT-3', and reverse 5'-GAGTCC TTCCACGATACCAA-3'; HIF1α forward, 5'-GGCGCGAAC GACAAGAAAAA-3', and reverse 5'-GGCTGTGTCGAC TGAGGAAA-3'.

Western blotting. Proteins were extracted using RIPA lysis buffer (cat. no. HY-K1001; MedChemExpress) from JEG-3 cells and MSCs-Ex. The concentration of the isolated protein was quantified via BCA Protein Assay kit (cat. no. 23225; Thermo Fisher Scientific, Inc.). Isolated proteins (5 μg) were mixed with 5X SDS-PAGE protein loading buffer (cat. no. 20315ES05; Shanghai Yeasen Biotechnology Co., Ltd.). Proteins (20 μg) were separated on 12% SDS-acrylamide gels, followed by transferring onto PVDF membranes, which were incubated with 5% non-fat milk for 1 h at room temperature, and with rabbit anti-HIF-1α (1:1,000; cat. no. ab179483; Abcam), rabbit anti-CD9 (1:1,000; cat. no. ab236630; Abcam), rabbit anti-CD81 (1:1,000; cat. no. ab79559; Abcam), rabbit anti-LAMP-2B (1:1,000; cat. no. ab18529; Abcam), rabbit anti-TSG101 (1:1,000; cat. no. ab125011; Abcam) and rabbit anti-GAPDH (1:10,000; cat. no. 10494-1-AP; ProteinTech Group, Inc.) overnight at 4˚C. Subsequently, membranes were incubated with horseradish peroxidase-conjugated mouse anti-rabbit IgG (1:5,000; cat. no. BM2006; Boster Biological Technology) for 1 h at room temperature. Protein bands were determined via ECL western blot detection reagents (Thermo Fisher Scientific, Inc.). The protein gray value was calculated using ImageJ (Version 1.5.3; National Institutes of Health).

Glucose uptake and lactate production. Transfected JEG-3 cells were seeded in six-well plates at the concentration of $3x10^5$/well. After culturing at 37˚C for 48 h, the cells were collected and lysed with Cell and Tissue Lysis Buffer for Glucose Assay (cat. no. S3062; Beyotime Institute of Biotechnology). The samples were then centrifuged at 1,200 x g at 4˚C for

10 min to obtain the supernatant of cells. The glucose concentration in the supernatant was determined using the glucose oxidase method (Amplex Red Glucose/Glucose Oxidase Assay kit; cat. no. MP 22189; Invitrogen; Thermo Fisher Scientific, Inc.). An appropriate amount of 1X reaction buffer was added to dilute 400 mM glucose to produce a glucose concentration of 0-200 μM to make the standard curve. Subsequently, 50 μl of each standard, controls and samples were added to the individual wells of the microplate in duplicate. The absorbance at OD 590 nm was measured using a microplate reader (LT-4000; Labtech International Ltd,).

The lactate in the supernatant was measured according to the instructions of the Lactate Detection kit (cat. no. K607-100; BioVision; Abcam). A total of 10 μl samples, 90 μl distilled water, 40 μl reagent 2 and 60 μl chromogen solution were added to the well and mixed thoroughly. Then the wells were incubated at 37˚C in dark for 30 min followed by measuring the absorbance at 530 nm.

Cell viability assay using Cell Counting Kit-8 (CCK-8). Transfected JEG-3 cells were passed onto the 96-well plates ($1x10^3$ cells/well) and cultured in an incubator for 24, 48, 72, 96 and 120 h at 37˚C. Next, CCK-8 regent (10 μl/well; cat. no. A311-01; Vazyme Biotech Co., Ltd.) was added to the cells and kept at 37˚C for 3 h. Eppendorf BioPhotometer® D30 (Eppendorf) was used to acquire the values of absorbance at 450 nm. The cell viability was calculated from the absorbance values for five consecutive days. The cell viability percentage was calculated as follows: Cell viability (%)=(sample absorbance/control absorbance) x100.

Cell invasion assay. Transwell assay was conducted to measure the changes in JEG-3 cells invasion after HIF1α lentivirus transfection. Transwell chambers (cat. no. 3402; Corning Life Sciences) were pre-coated with Matrigel (cat. no. 356234; Corning Life Sciences) for 6 h at 37˚C. A 150-μl JEG-3 cell suspension in serum-free DMEM was seeded in the upper layer of the six-well Transwell chamber ($7x10^3$ cells/well). In addition, 600 μl DMEM containing 10% FBS was added to the lower chamber. After 48 h incubation at 37˚C, JEG-3 cells on the basolateral chamber were washed twice using PBS, and stained with 1% crystal violet for 30 min at room temperature. JEG-3 cells were visualized and images were captured under the light microscope (magnification, x200; Olympus cX2; Olympus Corporation) after washing using PBS twice.

Mesenchymal stem cells (MSCs) identification. MSCs were obtained from Procell Life Science & Technology Co., Ltd. (cat. no. CP-H166), which were primary human MSCs that have not been immortalized. The cells were kept in DMEM medium adding 10% FBS and 100 U/ml penicillin and streptomycin. Then the surface markers of the cultured MSCs were identified using CD90 and CD44 by immunofluorescence assays. MSCs were plated in a 35-mm confocal dish and cultured for 48 h followed by fixing with 4% paraformaldehyde for 20 min at room temperature. After rinsing with PBS, cells were permeabilized with 0.5% Triton X100 in PBS and blocked with 3% BSA for 1 h at room temperature. Cells were then incubated overnight with anti-CD44 (1:50; cat. no. 15675-1-AP; ProteinTech Group, Inc.), anti-CD90 (1:50; cat. no. 66766-1-Ig; ProteinTech Group, Inc.), anti-CD34 (1:50; cat. no. 60287-1-Ig; ProteinTech Group, Inc.) and anti-CD45 (1:50; cat. no. 14486-1-AP; ProteinTech Group, Inc.) antibodies at 4˚C followed by 2 h incubation with goat anti-mouse IgG (H+L) Cy3-conjugated and goat anti-rabbit IgG (H+L) FITC-conjugated secondary antibodies (1:100; cat. no. BA1031 and BA1105, respectively; Boster Biological Technology). After three TBS-0.05% Tween-20 washing steps, cells were incubated with DAPI (cat. no. D1306; Thermo Fisher Scientific, Inc.) for 10 min at 37˚C. Finally, cells were observed using Olympus fluorescence microscope BX53 (Olympus Corporation). The positive rate was calculated using the following formula: Positive rate=(number of positive cells/number of total cells) x100%. The cell number were analyzed using ImageJ software (1.4; National Institutes of Health).

Homing peptide, sh-HIF1α peptide nucleic acid conjugates. The LAMP-2B + 5'-TGTTGTGGTAAACGTAAA-3' (gene sequence of CCGKRK) gene was amplified from cDNA template by PCR, then purified and recovered with a gel recovery kit (Beijing Solarbio Science & Technology Co., Ltd.). The gene was subsequently cloned and ligated to the GV493 vector (hU6-MCS-CBh-MCS-IRES-puromycin; Shanghai GeneChem Co., Ltd.). A 3rd generation system was used to package the lentivirus. Additionally, an sh-HIF1α sequence (5'-ACGACAAGAAAAAGATAAGTT-3') was also ligated into the same GV493 vector using an independent promoter. Upon transduction into cells, the lentiviral particles generated in this manner facilitated the overexpression of both LAMP-2B + CGKRK and HIF1α shRNA. The vectors (100 nM) and packaging plasmids (vector:packaging vector:envelope ratio, 10:3:1) were co-transfected into $1x10^6$ 293T cells with Lipofectamine 2000 at 37˚C for 8 h. The sh-HIF1α-LAMP-2B lentivirus and negative control (empty vector) were collected and filtered through a 0.45 μM filter after 293T cells were cultured at 37˚C for 3 days. MSCs were then transduced with lentiviral vectors at a MOI of 10 for 8 h followed by replacement with fresh medium. MSCs were cultured at 37˚C for 48 h and subsequently treated with puromycin (1 μg/ml) for 48 h to select stably transduced cells, 0.5 μg/ml puromycin was used for maintenance.

Isolation of exosomes. MSCs supernatant was collected and centrifugated at 2,000 x g for 30 min at 4˚C. Following being filtered through 0.22 μm syringe filter (cat. no. SLGVR13SL; MilliporeSigma), which was further centrifuged at 120,000 g overnight at 4˚C using Optima XPN-100 high-speed freezing centrifuge (cat. no. CP100MX; Hitachi, Ltd.). Exosomes were precipitated from the supernatants. The sediments of exosomes were resuspended by cold PBS, and ultracentrifuged again at 120,000 x g for 90 min at 4˚C. The final sediments of exosomes were resuspended in cold PBS or SDT lysate buffer, and immediately stored at -80˚C.

Pep-sh-HIF1α and exosomes binding. Exosomes (30 g) were preincubated with LAMP-2B-CCGKRK-sh-HIF1α peptide (30 g) overnight at 4˚C, followed by washing with PBS five times in 2-ml ultracentrifuge tubes and filtration with 100-kDa diafiltration tube (MilliporeSigma) to remove

unbound peptides. Subsequently, peptide-exosome complexes (30 g) were incubated with 4-mm aldehyde/sulfate latex beads (Invitrogen; Thermo Fisher Scientific, Inc.) for 15 min at room temperature under rotation followed by washing with PBS for three times. Then recovered beads were subjected to various tests.

Transmission electron microscopy. Purified exosomes supernatant was resuspended PBS. The exosome pellets were fixed with 2.5% glutaraldehyde for 1 h at room temperature, and post-fixed with 1% osmium for 1 h at room temperature. A total of 20 μl exosomes suspensions were added onto copper grid carefully, blotted up and stained with 2% phosphotungstic acid (PTA) for 2 min at room temperature. Sample was imaged using a transmission electron microscope (cat. no. HT-7700; Hitachi, Ltd.).

Nanoparticle tracking analysis. Isolated exosome was diluted to 1 ml in TBS with 0.1% Pluronic F-68 and 2 mmol/l EDTA for the next analysis. Size of exosomes was determined using Nanosight Tracking Analysis by utilizing nanoparticle tracking analysis (NTA; N30E; NanoFCM, Inc.) referring to the documented protocol (17).

Flow cytometry. To characterize individual exosomes by flow cytometry, exosomes were labeled with 1,1'-dioctadecyltetramethyl indotricarbocyanine iodide (cat. no. DL22065, Duolaimi Biotechnology Co., Ltd.), which labels the lipid in exosomes, as per the manufacturer's instruction and subjected to flow cytometry. To measure the percentage of pep-positive exosomes in total exosomes, DiR-labeled exosomes (5 g) were incubated with homing peptide (CCGKRK)-labeled anti-mouse antibody (1:20) generated in collaboration with NovoPro Bioscience, Inc. in 4% BSA for 30 min at 4˚C, followed by 1:10 dilution with PBS, and were analyzed with flow cytometry (FACSCalibur; BD Biosciences). Uncoated beads were used as negative controls for gating.

Statistical analysis. Statistical analysis was conducted using GraphPad Prism software (8.0; GraphPad Software, Inc.). All experiments were repeated thrice and data in the present study are presented as with mean ± standard deviation. Kolmogorov-Smirnov testing for normality of distribution was used to determine if variables were parametric or non-parametric. Unpaired Student's t-test was used for two group parametric comparisons, and one-way ANOVA followed by Tukey's post hoc test was used for multiple parametric comparisons. Mann-Whitney U testing was used for nonparametric variables. $P<0.05$ was considered to indicate a statistically significant difference.

Results

Expression level of HIF1α in trophoblast cells. HIF1α was overexpressed in JEG-3 cells via lentiviral transfection. Fluorescence microscopy confirmed high efficiencies of lentivirus transfection with a large proportion of GFP-positive cells (Fig. 1A). Analysis of both mRNA and protein levels revealed a significant increase of HIF1α in the transfected cells when compared with the control group detected by RT-qPCR and western blotting (Fig. 1B-D).

HIF1α promotes aerobic glycolysis and decreased the invasion capacity of trophoblast cells. Elevated HIF1α in JEG-3 cells led to a significant increase in glucose uptake compared with the NC group (Fig. 2A). Additionally, there was a significant elevation in lactate production in HIF1α-overexpressed JEG-3 cells (Fig. 2B). Overexpression of HIF1α significantly enhanced the proliferation ability of JEG-3 cells (Fig. 2C). Moreover, increased expression of HIF1α significantly suppressed the invasion ability of JEG-3 cells via Transwell invasion assays (Fig. 2D). These observations suggested that HIF1α was associated with the invasion and aerobic glycolysis of JEG-3 cells.

Observation and identification of human MSCs. CD44 and CD90 are cell surface markers that are expressed by human MSCs (27). The present study demonstrated that the MSCs bought from Procell Life Science & Technology Co., Ltd. were spindle-shaped (fibroblast-like cells), which is typical morphology of MSCs. Results of immunofluorescence assay indicated that both CD90-positive and CD44-positive rates of MSCs were ~100%, while lacking CD34 and CD45 human leukocyte markers (Fig. 3A). The results revealed that the purity of the isolated MSCs was high enough for the subsequent experiments.

Characterization of isolated exosomes. The exosomes harvested from the supernatant of MSCs were characterized using electron microscopy, which demonstrated a presence of small membrane-bound vesicles (Fig. 4A). This observation is consistent with the typical morphology of exosomes (28). The majority of the population was in the size range of 50-130 nm in diameter (Fig. 4A), which is consistent with previously reported features of exosomes (29). Western blotting was applied to determine the level of the typical exosomal markers CD9 antigen (CD9), CD81 antigen (CD81), exosomal protein LAMP-2B and tumor susceptibility gene 101 (TSG101) (30). As expected, the exosomal markers, including CD63, CD81, LAMP-2B and TSG101, were enriched in exo-NC and exo-pep-sh-HIF1α compared with those in cells (Fig. 4B). Approximately 69.94% of exosomes were labeled by DiR, and ~87.56% of DiR-labeled exosomes were modified with homing peptide (CCGKRK) demonstrated by flow cytometry exosomes (Fig. 4C). These findings support the conclusion that the homing peptide successfully binds to exosomes LAMP-2B.

HIF1α knockdown of MSCs-derived exosomes increases the invasion capacity of trophoblast cells. Next, HIF1α levels in MSC-Ex-treated JEG-3 cells were tested. The RT-qPCR assay revealed that the HIF1α level in MSC-Ex-treated JEG-3 cells was significantly decreased compared with the exo-NC group (Fig. 5A). In addition, HIF1α protein level in HIF1α-silenced MSC-Ex-treated JEG-3 cells was also significantly suppressed (Fig. 5B). Knockdown of HIF1α significantly enhanced the invasion ability of trophoblast JEG-3 cells (Fig. 5C), which plays an important role in embryo implantation.

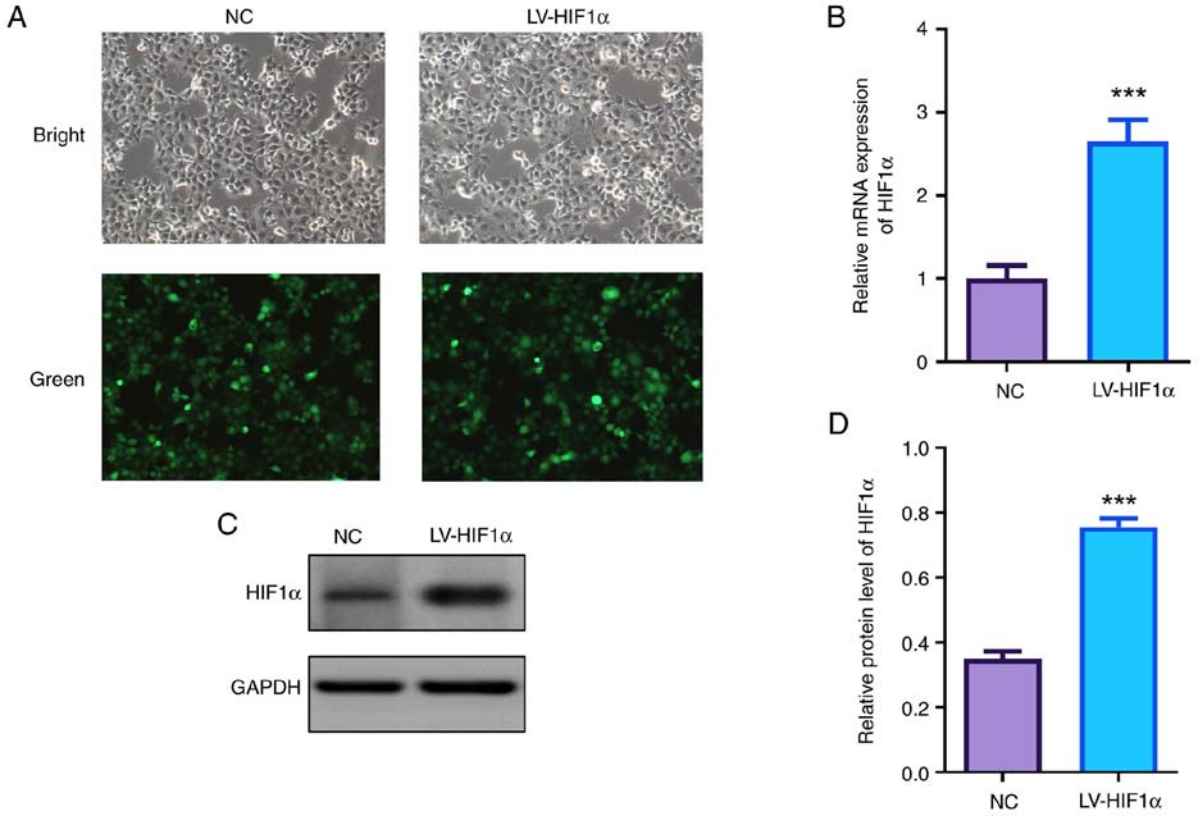

Figure 1. HIF1α is overexpressed in JEG-3 cells. (A) Transfection efficiency of HIF1α-overexpressing lentivirus was detected using immunofluorescence (magnification, x100). (B) mRNA and (C) protein levels of HIF1α in JEG-3 cells were determined using reverse transcription-quantitative PCR and western blotting, respectively. (D) Grayscale analysis was performed using ImageJ software. ***P<0.001 compared with NC. HIF1α, hypoxia-inducible factor-1α; NC, negative control; lv, lentiviral.

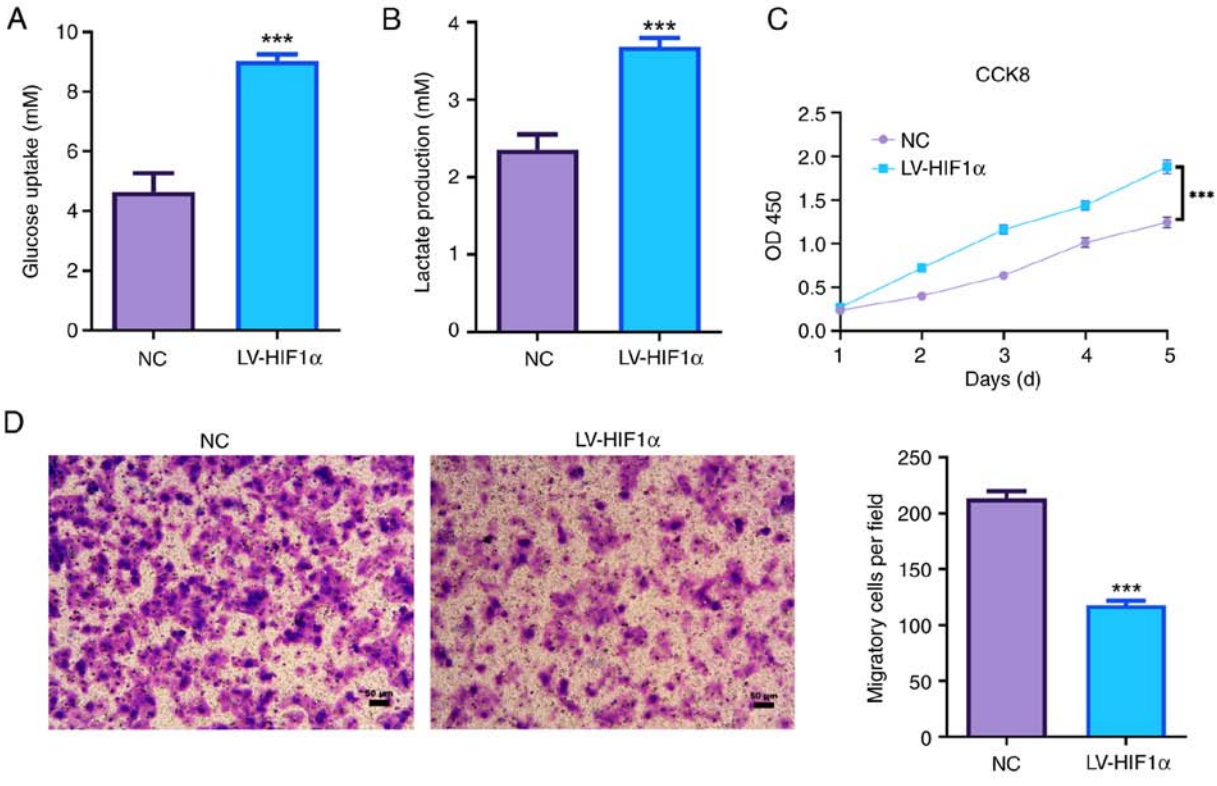

Figure 2. HIF1α promotes aerobic glycolysis and decreases the invasion capacity of JEG-3 cells. (A) Glucose concentration in the supernatant of JEG-3 cells was determined using a Glucose Oxidase Assay kit. (B) Lactate in JEG-3 cells supernatant was measured via Lactate Detection kit. (C) Viability of JEG-3 cells was detected using CCK-8. (D) Invasion capability of JEG-3 cells was determined using Transwell. ***P<0.001 compared with NC. HIF1α, hypoxia-inducible factor-1α; NC, negative control; lv, lentiviral; CCK-8, Cell Counting Kit-8.

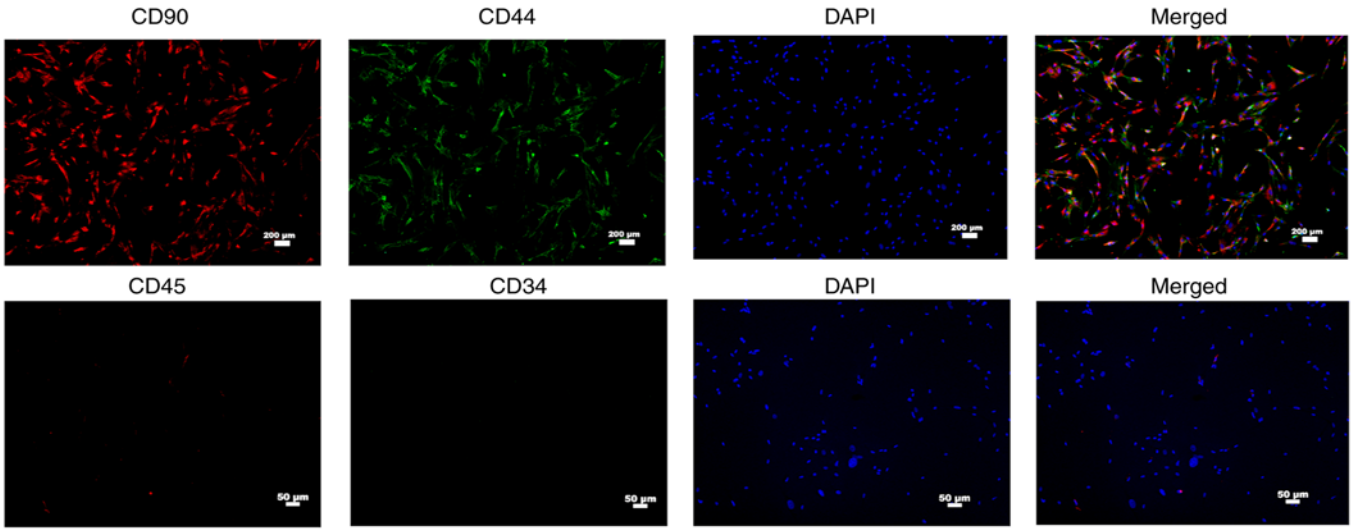

Figure 3. Identification of human MSCs. Representative fluorescence images of CD90-/CD44-positive and CD45-/CD34-negative MSCs. Scale bar, 200 μm. CD90, red; CD44, green; DAPI, blue. MSCs, mesenchymal stem cells.

Discussion

PE is often linked to reduced invasiveness of fetal trophoblast cells, leading to inadequate uterine placental perfusion (31). Sustained hypoxia leads trophoblasts to fail to differentiate from a proliferative to an invasive phenotype after 9 weeks of gestation, resulting in failed implantation (23,32). The current study conjugated an anchor peptide specific CCG ligand (CCGKRK) to exosomal membrane protein LAMP-2B to target HIF1α deletion exosomes to the placenta, which significantly enhanced the invasion ability of trophoblast. The results unveil new potential therapeutic targets for the prevention and treatment of PE.

At present, there are no effective treatments for PE. The few drugs licensed for pregnancy disorders often lead to serious systemic toxicity as their low molecular weights cross the placenta from mother to fetus (33,34). Thus, developing targeted therapies will be a highly effective therapeutic strategy for PE. HIF1α, a key regulator of intracellular oxygen metabolism, plays an important role in the development of the tumor (35). HIF1α is significantly upregulated to maintain trophoblasts in a proliferative, non-invasive and immature phenotype, which share some similarities with tumor cells in the biological processes, during the initial phase of embryonic development (23,36). After that, oxygen levels in the intervillous spaces increase from 2% O_2 before 9 weeks to 8% O_2 at 10 to 12 weeks of pregnancy (37). Correspondingly, HIF1α are rapidly reduced after 9 weeks of gestation. However, preeclamptic women have significantly higher oxidative stress and serum HIF1α levels compared with normal pregnant women, which leads the trophoblasts development to remain arrested at an immature stage, causing inadequate trophoblast invasion (38,39). HIF1α-overexpressed pregnant mice have significantly elevated blood pressure, decreased placental weights and histopathological placental abnormalities (40). Serum HIF1α levels have already been used to predict PE (23). In the present study, upregulated HIF1α was confirmed to significantly promote the proliferation while suppressing the invasion of trophoblast cells. This suggested that HIF1α deletion might be a potential therapeutic possibility for PE.

Moreover, PE is implicated in abnormal glucose and lipid metabolism (41-43). Gestational diabetes mellitus is one of the most common and important complications of pregnancy (44). Chronic fetal hypoxia causes deficits in oxidative glucose metabolism and enhancement of glycolytic metabolism, which causes energy production via glucose oxidation to be replaced by glycolysis (43). This abnormal aerobic glycolysis is also called metabolic reprogramming, a phenomenon known as the Warburg Effect, which is a hallmark of cancer, such as breast cancer, gastric cancer and colorectal cancer (45-47). However, a potential role for aerobic glycolysis in PE has not been elucidated. HIF1α facilitates glucose transporters and glycolytic enzymes expression that promote glucose uptake and glycolysis in Th17 cells (48). Thus, elevated levels of HIF1α in the hypoxic microenvironments at 10 to 12 weeks of gestation might mean trophoblasts fail to switch to an invasive phenotype by promoting aerobic glycolysis. The present study revealed that HIF1α overexpression promoted the uptake of glucose and the production of lactate in trophoblast cells. However, HIF-1α overexpression led to increased proliferation of trophoblast cells. The enhanced glucose and lactate production did not definitively exclude the possibility of cell proliferation-induced promotion. Thus, the enhanced glucose and lactate production resulted from increasing cell number or upregulation of HIF-1α overexpression needs further investigation.

Disrupting the expression of disease-causing genes by gene editing is already a well-established technique (49). However, the method to achieving efficient intervention of HIF1α expression in the placenta needs to be investigated. In recent years, several research reports have focused on delivering therapeutic drugs specifically to the placenta via nanoparticles, which exert high chemical stability, high drug loading capacity and low toxicity (50,51). Notably, extensive studies have confirmed the positive effects of MSCs on PE (11,52-54). In various PE rat models, MSC transplantation improves PE symptoms and

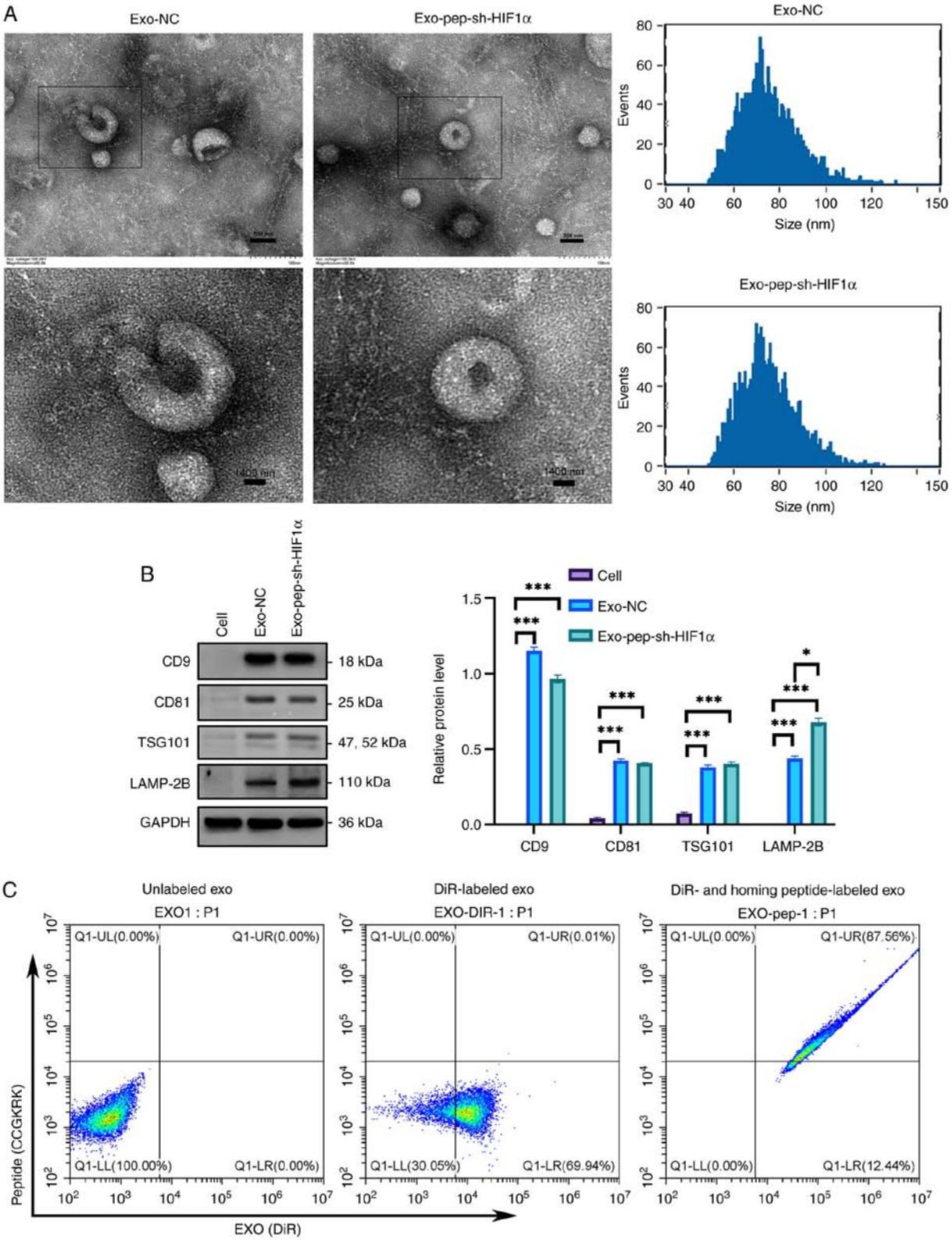

Figure 4. Characterization of exosomes after isolation. (A) Electron micrographs of exosomes isolated from MSCs. NTA (NanoSight) was applied to determine the size distribution of isolated exosomes in diameter. (B) Western blotting was performed for the indicated proteins. Grayscale analysis was performed by ImageJ software. (C) Flow cytometry for measuring the modification efficiency of placental homing peptide CCGKRK on exosomes. DiR-labeled exosomes (5 g) and homing peptide (CCGKRK)-labeled anti-mouse antibody were used. *P<0.05 and ***P<0.001. MSCs, mesenchymal stem cells; NC, negative control; sh-, short hairpin; TSG101, tumor susceptibility gene 101; LAMP-2B, lysosome-associated membrane glycoprotein 2b; HIF1α, hypoxia-inducible factor-1α.

inhibits inflammatory cytokines such as TNF-α and IL-6, providing evidence that human umbilical cord-derived MSCs may be a possible therapy for preeclampsia (53,55,56). MSCs exert their therapeutic functions via secretion of bioactive products, namely the exosomes, which have a high biocompatibility, low toxicity and low immunogenicity that makes them

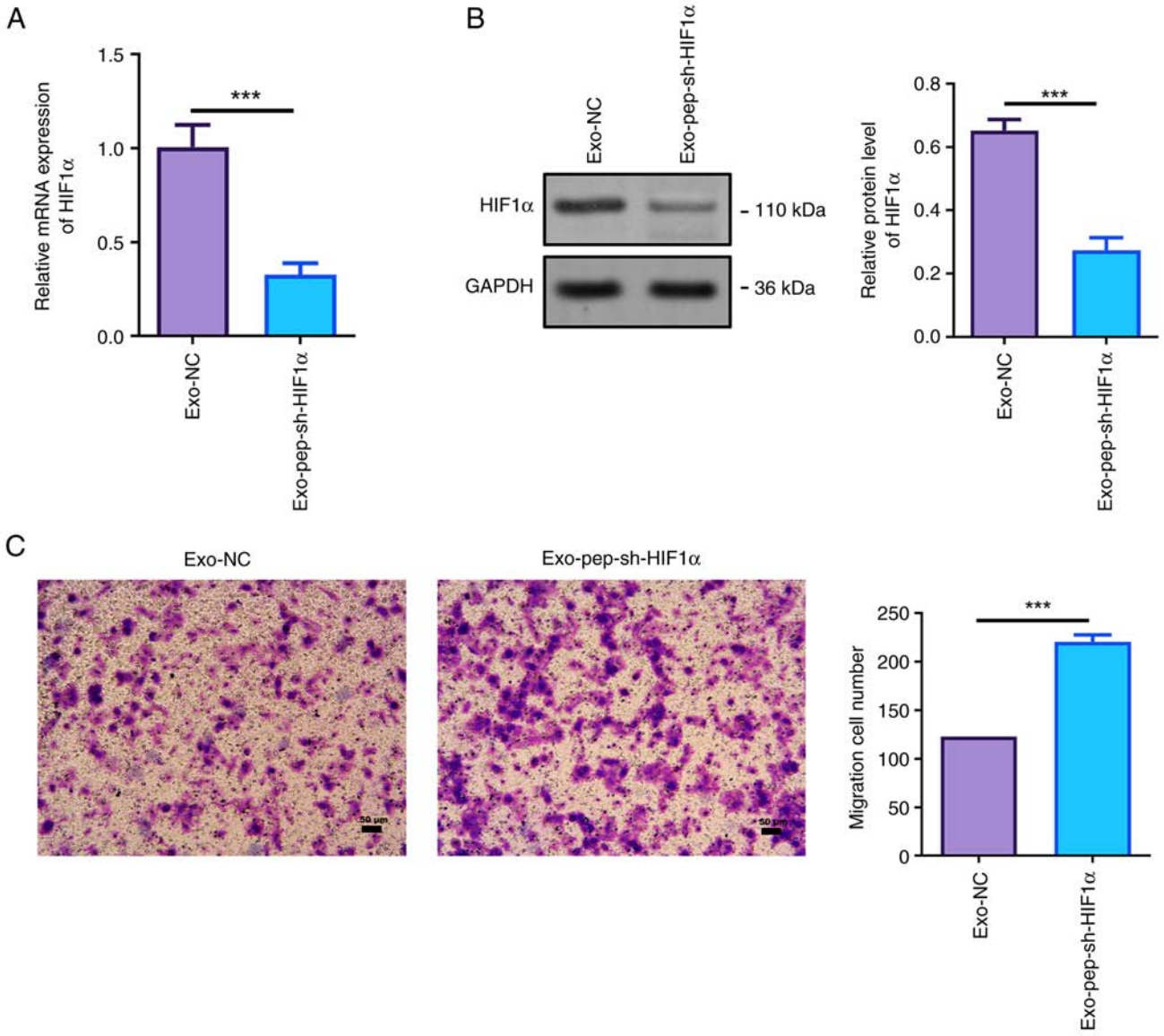

Figure 5. Exo-pep-sh-HIF1α facilitates placental invasion. The level of HIF1α in Exo-pep-sh-HIF1α treated JEG-3 cells was determined by (A) reverse transcription-quantitative PCR and (B) western blotting. Grayscale analysis was performed by ImageJ software. (C) Invasion capability of Exo-pep-sh-HIF1α treated JEG-3 cells was determined by Transwell (magnification, x100). ***P<0.001. HIF1α, hypoxia-inducible factor-1α; NC, negative control; sh-, short hairpin.

ideal drug delivery carriers of anti-PE drugs (57). The present study succeeded in conjugating CCG ligand (CCGKRK) to the exosomal membrane protein LAMP-2B, which led MSCs-derived exosomes to target the placenta. In the present study, MSC exosomes were used as a biocompatible drug carrier to target HIF1α siRNA to the placenta. To the best of our knowledge, this is the first attempt to make exosomes target placental tissue by genetic engineering. Notably, silencing HIF1α encouraged an aggressive phenotype that facilitated trophoblasts invasion, suggesting that HIF1α deletion is a potent way to interfere with the progression of PE. Clinically, some factors can be used to predict PE (58). If it poses a high risk of PE, some measures can be taken to intervene PE in advance, such as enhancing the invasion ability of trophoblasts by carrying sh-HIF1α to placenta by exosomes before PE is diagnosed.

There were some pitfalls and drawbacks in present study. Firstly, the experiments *in vitro* were only conducted in JEG3 cells, a commonly used choriocarcinoma cell line that serves as a model of villous trophoblast cells, whereas immortalized human chorionic trophoblast cells such as HTR-8 cells are considered to be an improved cell model to study trophoblast function. Therefore, further studies should be conducted using HTR-8 cells to confirm the findings presented in this study. Additionally, due to limited experimental conditions, the feasibility and effectiveness of targeted delivery of HIF1α deletion exosomes to the placenta by conjugating CCG ligand (CCGKRK) to LAMP-2B in animal models or human tissue samples has not yet been confirmed. In the present study, knockdown of HIF1α was proposed as a potential treatment to increase trophoblast invasion. However, it is essential to consider the potential effects of HIF1α knockdown on early pregnancy processes, such as implantation and placental development. Therefore, targeted and precise control of HIF1α knockdown is necessary to avoid any adverse effects on these critical events. Further research is required to elucidate the underlying mechanisms and optimize the therapeutic

approach to ensure the safety and efficacy of HIF knockdown in the context of pregnancy complications.

In summary, the present study facilitated the targeted delivery of HIF1α deletion exosomes to the placenta by conjugating CCG ligand (CCGKRK) to LAMP-2B, and provided a novel platform for the development of placenta-specific therapeutics. Silencing HIF1α was confirmed to be an effective therapeutic target for PE by promoting trophoblast invasion.

Acknowledgements

Not applicable.

Funding

This study was supported by Hainan Provincial Natural Science Foundation of China (no. 821MS128 and 822MS164) and National Natural Science Fund Cultivating 530 Project of Hainan General Hospital (grant no. 2021MSXM04). Scientific research project of health industry in Hainan Province (grant no. 22A200234).

Availability of data and materials

All data generated or analyzed during this study are included in this published article.

Authors' contributions

FC and HC conceived and designed this study. FC and DM carried out the analyses and also participated in the study design. HC wrote the manuscript. RF participated in the analysis of data and helped edit the manuscript. FC and HC confirm the authenticity of all the raw data. All authors read and approved the final manuscript.

Ethics approval and consent to participate

The medical ethics committee of Hainan General Hospital waives the requirement for authors to obtain ethical approval for the use of commercially available cells.

Patient consent for publication

Not applicable.

Competing interests

The authors declare that they have no competing interests.

References

1. Broumand F, Lak SS, Nemati F and Mazidi A: A study of the diagnostic value of Inhibin A Tests for occurrence of preeclampsia in pregnant women. Electronic Physician 10: 6186-6192, 2018.
2. Duley L: The global impact of pre-eclampsia and eclampsia. Semin Perinatol 33: 130-137, 2009.
3. Poon LC, Shennan A, Hyett JA, Kapur A, Hadar E, Divakar H, McAuliffe F, da Silva Costa F, von Dadelszen P, McIntyre HD, *et al*: The international federation of gynecology and obstetrics (FIGO) initiative on pre-eclampsia: A pragmatic guide for first-trimester screening and prevention. Int J Gynaecol Obstet 145 (Suppl 1): S1-S33, 2019.
4. Rahma H, Indrawan IWA, Nooryanto M, Rahajeng and Keman K: Effect of a black cumin (*Nigella sativa*) ethanol extract on placental angiotensin II type 1-receptor autoantibody (AT1-AA) serum levels and endothelin-1 (ET-1) expression in a preeclampsia mouse model. J Taibah Univ Med Sci 12: 528-533, 2017.
5. Belay Tolu L, Yigezu E, Urgie T and Feyissa GT: Maternal and perinatal outcome of preeclampsia without severe feature among pregnant women managed at a tertiary referral hospital in urban Ethiopia. PLoS One 15: e0230638, 2020.
6. Miller EC, Wilczek A, Bello NA, Tom S, Wapner R and Suh Y: Pregnancy, preeclampsia and maternal aging: From epidemiology to functional genomics. Ageing Res Rev 73: 101535, 2022.
7. Spradley FT, Palei AC and Granger JP: Immune mechanisms linking obesity and preeclampsia. Biomolecules 5: 3142-3176, 2015.
8. Li X, Song Y, Liu F, Liu D, Miao H, Ren J, Xu J, Ding L, Hu Y, Wang Z, *et al*: Long Non-coding RNA MALAT1 promotes proliferation, angiogenesis, and immunosuppressive properties of mesenchymal stem cells by inducing VEGF and IDO. J Cell Biochem 118: 2780-2791, 2017.
9. Oh S, Jang AY, Chae S, Choi S, Moon J, Kim M, Spiekerkoetter E, Zamanian RT, Yang PC, Hwang D, *et al*: Comparative analysis on the anti-inflammatory/immune effect of mesenchymal stem cell therapy for the treatment of pulmonary arterial hypertension. Sci Rep 11: 2012, 2021.
10. Burlacu A, Grigorescu G, Rosca AM, Preda MB and Simionescu M: Factors secreted by mesenchymal stem cells and endothelial progenitor cells have complementary effects on angiogenesis in vitro. Stem Cells Dev 22: 643-653, 2013.
11. Wang D, Na Q, Song GY and Wang L: Human umbilical cord mesenchymal stem cell-derived exosome-mediated transfer of microRNA-133b boosts trophoblast cell proliferation, migration and invasion in preeclampsia by restricting SGK1. Cell Cycle 19: 1869-1883, 2020.
12. Choi JH, Jung J, Na KH, Cho KJ, Yoon TK and Kim GJ: Effect of mesenchymal stem cells and extracts derived from the placenta on trophoblast invasion and immune responses. Stem Cells Dev 23: 132-145, 2014.
13. Hosseini R, Asef-Kabiri L, Yousefi H, Sarvnaz H, Salehi M, Akbari ME and Eskandari N: The roles of tumor-derived exosomes in altered differentiation, maturation and function of dendritic cells. Mol Cancer 20: 83, 2021.
14. Li T, Yan Y, Wang B, Qian H, Zhang X, Shen L, Wang M, Zhou Y, Zhu W, Li W and Xu W: Exosomes derived from human umbilical cord mesenchymal stem cells alleviate liver fibrosis. Stem Cells Dev 22: 845-854, 2013.
15. Bjorge IM, Kim SY, Mano JF, Kalionis B and Chrzanowski W: Extracellular vesicles, exosomes and shedding vesicles in regenerative medicine-a new paradigm for tissue repair. Biomater Sci 6: 60-78, 2017.
16. Gatti S, Bruno S, Deregibus MC, Sordi A, Cantaluppi V, Tetta C and Camussi G: Microvesicles derived from human adult mesenchymal stem cells protect against ischaemia-reperfusion-induced acute and chronic kidney injury. Nephrol Dial Transplant 26: 1474-1483, 2011.
17. Hu Q, Yao J, Wu X, Li J, Li G, Tang W, Liu J and Wan M: Emodin attenuates severe acute pancreatitis-associated acute lung injury by suppressing pancreatic exosome-mediated alveolar macrophage activation. Acta Pharm Sin B 12: 3986-4003, 2022.
18. Kojima R, Bojar D, Rizzi G, Hamri GC, El-Baba MD, Saxena P, Ausländer S, Tan KR and Fussenegger M: Designer exosomes produced by implanted cells intracerebrally deliver therapeutic cargo for Parkinson's disease treatment. Nat Commun 9: 1305, 2018.
19. Bai J, Duan J, Liu R, Du Y, Luo Q, Cui Y, Su Z, Xu J, Xie Y and Lu W: Engineered targeting tLyp-1 exosomes as gene therapy vectors for efficient delivery of siRNA into lung cancer cells. Asian J Pharm Sci 15: 461-471, 2020.
20. Hu C, Chen X, Huang Y and Chen Y: Co-administration of iRGD with peptide HPRP-A1 to improve anticancer activity and membrane penetrability. Sci Rep 8: 2274, 2018.
21. Beards F, Jones LE, Charnock J, Forbes K and Harris LK: Placental homing Peptide-microRNA inhibitor conjugates for targeted enhancement of intrinsic placental growth signaling. Theranostics 7: 2940-2955, 2017.
22. Burton GJ, Hempstock J and Jauniaux E: Nutrition of the human fetus during the first trimester-a review. Placenta 22 (Suppl A): S70-S77, 2001.
23. Tianthong W and Phupong V: Serum hypoxia-inducible factor-1alpha and uterine artery Doppler ultrasound during the first trimester for prediction of preeclampsia. Sci Rep 11: 6674, 2021.

24. Zhao H, Wong RJ and Stevenson DK: The impact of hypoxia in early pregnancy on placental cells. Int J Mol Sci 22: 9675, 2021.
25. Mol BWJ, Roberts CT, Thangaratinam S, Magee LA, de Groot CJM and Hofmeyr GJ: Pre-eclampsia. Lancet 387: 999-1011, 2016.
26. Livak KJ and Schmittgen TD: Analysis of relative gene expression data using real-time quantitative PCR and the 2(-Delta Delta C(T)) method. Methods 25: 402-408, 2001.
27. Lan T, Luo M and Wei X: Mesenchymal stem/stromal cells in cancer therapy. J Hematol Oncol 14: 195, 2021.
28. Ma L, Wei J, Zeng Y, Liu J, Xiao E, Kang Y and Kang Y: Mesenchymal stem cell-originated exosomal circ-DIDO1 suppresses hepatic stellate cell activation by miR-141-3p/PTEN/AKT pathway in human liver fibrosis. Drug Deliv 29: 440-453, 2022.
29. Huang C, Tang S, Shen D, Li X, Liang L, Ding Y and Xu B: Circulating plasma exosomal miRNA profiles serve as potential metastasis-related biomarkers for hepatocellular carcinoma. Oncol Lett 21: 168, 2021.
30. Liu YM, Tseng CH, Chen YC, Yu WY, Ho MY, Ho CY, Lai MMC and Su WC: Exosome-delivered and Y RNA-derived small RNA suppresses influenza virus replication. J Biomed Sci 26: 58, 2019.
31. Yang P, Dai A, Alexenko AP, Liu Y, Stephens AJ, Schulz LC, Schust DJ, Roberts RM and Ezashi T: Abnormal oxidative stress responses in fibroblasts from preeclampsia infants. PLoS One 9: e103110, 2014.
32. Matsumoto L, Hirota Y, Saito-Fujita T, Takeda N, Tanaka T, Hiraoka T, Akaeda S, Fujita H, Shimizu-Hirota R, Igaue S, *et al*: HIF2α in the uterine stroma permits embryo invasion and luminal epithelium detachment. J Clin Invest 128: 3186-3197, 2018.
33. Kim MK, Lee SM, Oh JW, Kim SY, Jeong HG, Kim SM, Park CW, Jun JK, Hahn SK and Park JS: Efficacy and side effect of ritodrine and magnesium sulfate in threatened preterm labor. Obstet Gynecol Sci 61: 63-70, 2018.
34. Driul L, Londero AP, Adorati-Menegato A, Vogrig E, Bertozzi S, Fachechi G, Forzano L, Cacciaguerra G, Perin E, Miceli A and Marchesoni D: Therapy side-effects and predictive factors for preterm delivery in patients undergoing tocolysis with atosiban or ritodrine for threatened preterm labour. J Obstet Gynaecol 34: 684-689, 2014.
35. Mei T, Wang Z, Wu J, Liu X, Tao W, Wang S and Chen F: Expression of GLUT3 and HIF-1α in meningiomas of various grades correlated with peritumoral brain edema. Biomed Res Int 2020: 1682352, 2020.
36. Li J, Wu Y and Liu H: Expression and role of miR-338-3p in peripheral blood and placenta of patients with pregnancy-induced hypertension. Exp Ther Med 20: 418-426, 2020.
37. Jauniaux E, Watson A and Burton G: Evaluation of respiratory gases and acid-base gradients in human fetal fluids and uteroplacental tissue between 7 and 16 weeks' gestation. Am J Obstet Gynecol 184: 998-1003, 2001.
38. Iriyama T, Wang W, Parchim NF, Song A, Blackwell SC, Sibai BM, Kellems RE and Xia Y: Hypoxia-independent upregulation of placental hypoxia inducible factor-1α gene expression contributes to the pathogenesis of preeclampsia. Hypertension 65: 1307-1315, 2015.
39. Ali LE, Salih MM, Elhassan EM, Mohmmed AA and Adam I: Placental growth factor, vascular endothelial growth factor, and hypoxia-inducible factor-1α in the placentas of women with pre-eclampsia. J Matern Fetal Neonatal Med 32: 2628-2632, 2019.
40. Tal R, Shaish A, Barshack I, Polak-Charcon S, Afek A, Volkov A, Feldman B, Avivi C and Harats D: Effects of hypoxia-inducible factor-1alpha overexpression in pregnant mice: Possible implications for preeclampsia and intrauterine growth restriction. Am J Pathol 177: 2950-2962, 2010.
41. Ueki N, Takeda S, Koya D and Kanasaki K: The relevance of the Renin-Angiotensin system in the development of drugs to combat preeclampsia. Int J Endocrinol 2015: 572713, 2015.
42. Hu M, Li J, Baker PN and Tong C: Revisiting preeclampsia: A metabolic disorder of the placenta. FEBS J 289: 336-354, 2022.
43. Illsley NP, Caniggia I and Zamudio S: Placental metabolic reprogramming: Do changes in the mix of energy-generating substrates modulate fetal growth? Int J Dev Biol 54: 409-419, 2010.
44. Bosdou JK, Anagnostis P, Goulis DG, Lainas GT, Tarlatzis BC, Grimbizis GF and Kolibianakis EM: Risk of gestational diabetes mellitus in women achieving singleton pregnancy spontaneously or after ART: A systematic review and meta-analysis. Hum Reprod Update 26: 514-544, 2020.
45. Zhong D, Li Y, Huang Y, Hong X, Li J and Jin R: Molecular mechanisms of exercise on cancer: A bibliometrics study and visualization analysis via CiteSpace. Front Mol Biosci 8: 797902, 2021.
46. Xu Y, Lu J, Tang Y, Xie W, Zhang H, Wang B, Zhang S, Hou W, Zou C, Jiang P and Zhang W: PINK1 deficiency in gastric cancer compromises mitophagy, promotes the Warburg effect, and facilitates M2 polarization of macrophages. Cancer Lett 529: 19-36, 2022.
47. Jing Z, Liu Q, He X, Jia Z, Xu Z, Yang B and Liu P: NCAPD3 enhances Warburg effect through c-myc and E2F1 and promotes the occurrence and progression of colorectal cancer. J Exp Clin Cancer Res 41: 198, 2022.
48. Zhang Q, Wang L, Jiang J, Lin S, Luo A, Zhao P, Tan W and Zhang M: Critical role of AdipoR1 in regulating Th17 cell differentiation through modulation of HIF-1α-dependent glycolysis. Front Immunol 11: 2040, 2020.
49. Sun J, Carlson-Stevermer J, Das U, Shen M, Delenclos M, Snead AM, Koo SY, Wang L, Qiao D, Loi J, *et al*: CRISPR/Cas9 editing of APP C-terminus attenuates β-cleavage and promotes α-cleavage. Nat Commun 10: 53, 2019.
50. Zhang B, Tan L, Yu Y, Wang B, Chen Z, Han J, Li M, Chen J, Xiao T, Ambati BK, *et al*: Placenta-specific drug delivery by trophoblast-targeted nanoparticles in mice. Theranostics 8: 2765-2781, 2018.
51. Li L, Yang H, Chen P, Xin T, Zhou Q, Wei D, Zhang Y and Wang S: Trophoblast-targeted nanomedicine modulates placental sFLT1 for preeclampsia treatment. Front Bioeng Biotechnol 8: 64, 2020.
52. Chu Y, Chen W, Peng W, Liu Y, Xu L, Zuo J, Zhou J, Zhang Y, Zhang N, Li J, *et al*: Amnion-derived mesenchymal stem cell exosomes-mediated autophagy promotes the survival of trophoblasts under hypoxia through mTOR pathway by the downregulation of EZH2. Front Cell Dev Biol 8: 545852, 2020.
53. Zhang D, Fu L, Wang L, Lin L, Yu L, Zhang L and Shang T: Therapeutic benefit of mesenchymal stem cells in pregnant rats with angiotensin receptor agonistic autoantibody-induced hypertension: Implications for immunomodulation and cytoprotection. Hypertens Pregnancy 36: 247-258, 2017.
54. Qu HM, Qu LP, Pan XZ and Mu LS: Upregulated miR-222 targets BCL2L11 and promotes apoptosis of mesenchymal stem cells in preeclampsia patients in response to severe hypoxia. Int J Clin Exp Pathol 11: 110-119, 2018.
55. Wang LL, Yu Y, Guan HB and Qiao C: Effect of human umbilical cord mesenchymal stem cell transplantation in a rat model of preeclampsia. Reprod Sci 23: 1058-1070, 2016.
56. Fu L, Liu Y, Zhang D, Xie J, Guan H and Shang T: Beneficial effect of human umbilical cord-derived mesenchymal stem cells on an endotoxin-induced rat model of preeclampsia. Exp Ther Med 10: 1851-1856, 2015.
57. Xiong ZH, Wei J, Lu MQ, Jin MY and Geng HL: Protective effect of human umbilical cord mesenchymal stem cell exosomes on preserving the morphology and angiogenesis of placenta in rats with preeclampsia. Biomed Pharmacother 105: 1240-1247, 2018.
58. Stepan H, Galindo A, Hund M, Schlembach D, Sillman J, Surbek D and Vatish M: Clinical utility of sFlt-1 and PlGF in screening, prediction, diagnosis and monitoring of pre-eclampsia and fetal growth restriction. Ultrasound Obstet Gynecol 61: 168-180, 2023.